Transonic Airfoil Design Procedure Utilizing a Navier-Stokes Analysis Code

Naoki Hirose,* Susumu Takanashi,* and Nobuhiro Kawai†
National Aerospace Laboratory, Tokyo, Japan

An iterative procedure for transonic airfoil design utilizing a Navier-Stokes analysis code to attain arbitrarily specified pressure distributions is presented. The concept of the present design procedure depends on the fact that an inverse design method of the residual-correction type can be combined both with a Navier-Stokes analysis code for a wide range of flow regimes and with conventional full potential analysis codes. The logical validity of the concept is presented and numerical examples of supercritical and low-speed designs are presented. Since the Navier-Stokes code is used in the analysis mode of the procedure, shock wave and viscous effects (including trailing-edge separation), which are difficult to evaluate with the conventional potential design methods, are properly evaluated and effectively incorporated in the design procedure.

Introduction

RECENT progress in computational transonic aerodynamics has been remarkable. In the field of flow analysis methods, it has become feasible to compute the three-dimensional transonic flow around a full configuration of a realistic aircraft if the flow is assumed to be inviscid.[1,2] Viscous effects, such as the shock/boundary-layer interaction and trailing-edge separation, can be quantitatively evaluated by a time-averaged Navier-Stokes analysis code. Two-dimensional viscous transonic airfoil analysis with the Navier-Stokes equations is easily done within a reasonable computing time on the latest computers and gives reliable data on the aerodynamic characteristics for most practical aerodynamic design purposes.[3] Even a three-dimensional transonic flow analysis past a swept wing has become possible as the most advanced vector processing computers become available.[4]

Another effort in the field is the development of computational procedures in transonic aerodynamic design. Especially, transonic airfoil and wing design methods have been investigated by various researchers. Slooff[5] reviewed these methods and distinguishes between three different categories of such design procedures: indirect, inverse, and direct methods, although there may be different definitions of classification. Indirect methods are characterized by the fact that the designer has no control over either the aerodynamic quantities or the geometry. Hodograph and fictitious gas methods are among those. In most methods, the designer cannot arbitrarily specify the pressure distribution. Inverse methods are those that solve the classical inverse problem of aerodynamics. The designer specifies an arbitrary pressure distribution around an airfoil or wing and determines the geometry of the airfoil or the wing that realizes the given pressure distribution as the solution. In Slooff's definition, the direct methods mean design and optimization by the use of direct methods, i.e., flow analysis codes. He emphasizes especially the numerical optimization method in which a nonlinear optimization algorithm is linked with a flow analysis code to minimize or maximize some aerodynamic object function such as the lift-to-drag ratio.

Received May 17, 1985; presented as Paper 85-1592 at the AIAA 18th Fluid Dynamics and Plasmadynamics and Lasers Conference, Cincinnati, OH, July 16-18, 1985; revision received June 30, 1986.

*Branch Chief, Second Aerodynamics Division. Member AIAA.
†Senior Research Scientist, Second Aerodynamics Division.

The numerical optimization method in Slooff's last category has been investigated in recent years by Hicks[6] and others. One of the advantages of this method is the use of an available analysis code as a "black box" to give the gradients of the object function to the design variables. These design variables define the geometry of the airfoil or wing. When the number of the design variables is large, the number of calls to the analysis code is increased and the computing time becomes prohibitively large. Therefore, careful selection of the design variables describing a wide variety of geometries is the key to practical application of the method. A new cubic-spline wing parametrization using only four variables has been successfully proposed by Cosentino and Holst[7] to describe one wing section. Their method effectively applies to a design of the local, yet significant, part of the upper wing surface, excluding the leading- and trailing-edge regions. They use the quasi-Newton method optimization algorithm. The feasible direction method of Zoutendijk,[8] developed as the computer program CONMIN by Vanderplaats,[9] had previously been the only algorithm available for the nonlinear optimization with nonlinear constraints. Cosentino does not show how the constraints are treated in Cosentino-Holst's method. The existing papers dealing with numerical optimization cover only the use of the potential codes, although any flow analysis code (including the Navier-Stokes) may be linked with the numerical optimization algorithms. Computer efficiency may be one of the major reasons that no one has mentioned the possibility of utilization of Navier-Stokes codes in the past. Here, it is only noted that such utilization will soon become available to the researcher.

It is conjectured that the numerical optimization algorithm may be linked with the inverse methods when the target pressure distribution is used as the design variable. Because specification of the target pressure distribution imposes a heavy burden on the aerodynamicist to realize both good aerodynamic and boundary-layer characteristics with reasonable geometry, this combination seems quite promising, as Slooff predicts.

Among those three categories, the conventional inverse design methods are the most used. The inverse methods are subdivided into two categories. The first approach is the full inverse method based on full potential theory with a nonlinear Dirichlet boundary condition imposed on the unknown geometry. This requires numerical formulation different from flow analysis code and some iterative procedure to modify the starting presumed geometry until it satisfies the specified pressure distribution to be realized. Iterative inverse methods of this kind have been developed by Carlson[10] and Tranen[11]

for airfoils, Henne[12] for wings, and Shankar[13] for wing/body designs. The inverse formulations for the Euler and the Navier-Stokes equations will be very difficult and, to the authors' knowledge, are not yet presented in the open literature. Viscous effects may be incorporated through the use of coupling techniques for the inviscid/boundary-layer interaction.

The second approach of the inverse methods is a residual-correction procedure in which the residual (i.e., the difference between the actual and specified pressure distributions) is determined by the use of an analysis code and the geometry correction to compensate the residual is obtained from some approximate inverse procedure. As the geometry correction problem is based on some approximation, it requires several iterative steps between the flow analysis and geometry correction modes for the residual to converge to zero. This approach was used by Barger and Brooks,[14] Davis,[15] and McFadden[16] in their work on the design of a two-dimensional airfoil. The distinction between these three studies lies in the difference in their numerical formulation of the geometry correction problem. Takanashi[17] has developed a three-dimensional transonic wing design method based on this approach. The geometry correction problem is formulated in a three-dimensional integral equation form and is numerically solved. This design method is applicable to the global design of airfoils, i.e., geometry including both of the leading and trailing edges, and to the global and local spanwise design of wings. There is no restriction on the type of target pressure distributions. Pressure distributions with shock waves can be arbitrarily utilized, as well as the shockless pressure distributions with no additional constraints. Another advantage of the method is that the only information required for the geometry correction problem is the actual geometry coordinates, its pressure distribution, and the target pressure distribution. There is no need to modify the flow analysis code and it is genuinely treated as a "black box" to give the pressure distribution for a given geometry. As a result, the analysis code can be easily replaced with more advanced codes when they become available. Takanashi's method has been successfully applied to various transport-type wing designs for practical applications[18] using full potential flow analysis codes such as Jameson and Caughey's FLO-22[19] and FLO-27[20] and Boppe's transonic small-disturbance potential code for wing/body configurations.[21] Other residual-correction procedures suffer some greater or lesser disadvantages in solving the above-mentioned problems when compared with the present method.

The purpose of the present paper is to show that a (time-averaged) Navier-Stokes flow analysis code can be linked with Takanashi's inverse method to design transonic airfoils and to show that this procedure is effective for practical design purposes. In the past, no attempt has been made to formulate the Navier-Stokes equations inversely as a design problem or to utilize a Navier-Stokes analysis code in the design procedures as mentioned above. Full potential equation formulation has been used extensively in both full inverse and residual-correction methods. Although viscous effects may be incorporated to some extent by the use of the boundary-layer equations and the interaction coupling procedures for trailing edges and shock waves in the flow analysis code (see, e.g., Melnik et al.[22]), such procedures are more or less analytical and tedious in numerical formulation, and are not robust, and, therefore, are not necessarily applicable as a design method to every flow regime and its various pressure distributions. Most of such procedures fail when the shock wave strength is increased and the separation bubble at the foot of the shock wave grows or when the trailing-edge separation becomes noticeable. When a designer wants to pursue a very sophisticated airfoil design that reduces drag and realizes maximum lift and an increasing drag divergence Mach number, any deficiencies in the interaction coupling methods become important. Therefore, wind tunnel testing has been used in the iterative loop in the design procedure. When the computer-designed airfoil does not satisfy the required aerodynamic characteristics in the wind tunnel experiment, the designer has to go back to the computer design procedure. This is expensive in both time and money—a more efficient process must be sought.

Most of the factors leading to unsatisfactory performances are due to the viscous interaction effects. Even though attainment of the overall pressure distribution and lift coefficient may be easily satisfied by the inverse method without viscous coupling techniques, drag estimation is difficult to achieve even with such techniques because the pressure distribution in the vicinity of the trailing edge predicted by a potential design code differs from the experimental one—in some cases significantly. The empirical modification of trailing-edge pressure to accommodate to the boundary-layer computation is not a universal method and is numerically dependent, i.e., very sensitive to values of nonphysical numerical parameters. Therefore, the lift-to-drag ratio obtained by the design code often shows unrealistically excellent values, but is not reliable. The reader can refer to Ref. 23 for such an example. All such problems will be conquered, at least basically, by the introduction of the Navier-Stokes equations in the design procedure. To accomplish this, the design method must first have a logical validity for using Navier-Stokes equations within the procedure; the procedure then needs to be one that can easily adopt a Navier-Stokes analysis code without reformulation or modification; and, finally, the computing time must be reasonable.

In the following sections, the logical validity of the present design procedure utilizing a Navier-Stokes flow analysis code is described as an abstract examination; numerical examples of transonic airfoil design are then presented for both shockless and shock-containing pressure distributions. Low-speed design examples are also presented to show the limit of applicability of the present procedure. The computing time requirement is discussed in the light of the emerging vector processing computer programs.

Design Methodology

Concept of Design Procedure

The logical concept of the present design procedure is derived from a qualitative examination of relationship between the geometry and the pressure field. The exact proof and more details will be found in Refs. 17 and 24.

Let pressure field P be expressed as a function of geometry F, with flow Mach number M_∞ and Reynolds number Re as parameters in the real flow or its flow model (time-averaged), Navier-Stokes equations

$$P = \text{function } P(F; M_\infty, Re) \tag{1}$$

In the design problem, Eq. (1) is inverted and geometry F is expressed in terms of P,

$$F = \text{function } F(P; M_\infty, Re) \tag{2}$$

Provided Reynolds number Re is high and there is no or weak separation (even if the flow contains shock waves), geometry F can be estimated by an approximated geometry $\bar{F}$ governed by a submodel, the full potential equation with M_∞ as a parameter,

$$\bar{F} = \bar{F}(P; M_\infty) \tag{3}$$

Then, geometry F is expressed as

$$F = \bar{F} + \delta R \tag{4}$$

where R represents all of the higher-order terms and δ is a coefficient smaller than unity, $|\delta| \ll 1$.

From a practical point of view, function F may be a nonlinear and continuous function of P, M_∞, and Re, at least locally. For a small perturbation of the pressure field ΔP, the geometry is perturbed as ΔF from the original geometry F_0 and the new geometry F_{target} corresponding to a new pressure field is expressed as

$$F_{\text{target}} = F_0 + \Delta F_0 \tag{5}$$

where Δ represents a small perturbation and the subscript 0 represents the original value. Bringing the exact relation in Eq. (4) into the second term of Eq. (5) results in,

$$\begin{aligned} F_{\text{target}} &= F_0 + \left[\Delta \bar{F}_0 + \Delta(\delta R_0)\right] \\ &= F_0 + \Delta \bar{F}_0 + \delta \Delta R_0 \end{aligned} \tag{6}$$

Under the present assumptions, perturbation of all of the higher terms, ΔR_0, is small enough to be expressed as

$$\Delta R_0 = \epsilon R_0, \qquad |\epsilon| \ll 1 \tag{7}$$

Therefore,

$$F_{\text{target}} = F_0 + \Delta \bar{F}_0 + \delta \epsilon R_0 \tag{8}$$

As δ and ϵ are negligibly small, the primary part of the perturbation is $\Delta \bar{F}_0$. F_{target} can best be approximated by

$$F_{\text{target}} \doteq F_0 + \Delta \bar{F}_0 \tag{9}$$

The significant result of Eq. (9) is that only the perturbation term, i.e., the geometry correction term $\Delta \bar{F}_0$ is given by an approximated submodel, while the original geometry F_0 as well as P are expressed by any flow model governed by Eq. (1). In the conventional inverse methods, F_0 is also approximated by a full potential model $\bar{F}_0$. Therefore, the Navier-Stokes equations can be utilized in the present procedure as long as Eq. (9) is valid. It should be noted that the present argument can be applied to flow models such as the wind tunnel experiment and flight testing as well as to a wide range of various mathematical flow models.

Residual-Correction Procedure

Since Eq. (9) states only the relation between the geometry and its correction, an inverse design procedure of a residual-correction type must be constructed to obtain any numerical result. To utilize a Navier-Stokes analysis code in its original form, the present procedure is as follows. An arbitrary target pressure distribution P_{target} at a specified flow Mach number, angle of attack, and Reynolds number is chosen. The flowfield at the above flow condition is computed for an initial airfoil geometry F_0 using a Navier-Stokes code (analysis mode). The initial geometry may be chosen arbitrarily since the geometry correction will be made to the entire airfoil including both the leading and trailing edges. The pressure field P_0 for geometry F_0 is obtained, then the pressure difference from the target distribution ΔP_0 is checked if it has converged to zero. It is usual that for the initial guess of geometry the pressure difference is not negligible and the design mode, i.e., the geometry correction problem, is called to give the quantity of geometry correction $\Delta \bar{F}_0$. The Navier-Stokes code is again used to obtain new pressure distribution P_1 for the corrected geometry F_1. The pressure difference ΔP_1 is checked. The iterative loop between the analysis mode and the design mode is proceeded until the pressure difference becomes small. The details of each mode are described subsequently.

Geometry Correction Code

The derivation of the integral equation formulation of the geometry correction problem for airfoil and wing is briefly described herein. The details are found in Ref. 17. Since the argument is valid for both airfoil and wing and the numerical formulation for a three-dimensional wing was used in the numerical examples, the term wing is used throughout.

The three-dimensional full potential equation is written in terms of perturbation velocity potential ϕ. Assume a solution of ϕ for an initial geometry is obtained by means of an existing flow analysis code, see Eq. (1). If a perturbation $\Delta\phi$ from the known solution ϕ is introduced, the governing equation is expressed in terms of unknown $\Delta\phi$ and known solution ϕ with the flow tangency and boundary conditions on the pressure distribution on the wing surface. The geometry correction equation for $\bar{F}_0$ in terms of $\Delta\phi$ is obtained by making the reasonable assumption to neglect the higher-order terms. Applying Green's theorem, the perturbed equation is converted into an integrodifferential equation. After a little analytic manipulation and applying a decay function in the normal direction to the wing surface, the equation reduces to a simple two-dimensional integral equation for the wing surface. A unique solution is obtained with a trailing-edge closure condition enforced. This closure condition means that the correction of the trailing-edge thickness is zero, i.e., the trailing-edge thickness of the original wing remains unchanged. The original edge thickness, itself, need not be zero. This condition, however, does not necessarily mean that the resulting wing section contour has no crossing of the upper and lower surfaces along the chord from the leading to the trailing edge. Such a crossing, if it occurs, does not give a physically reasonable wing section. The target pressure distribution must be modified in order to obtain a physically reasonable wing section for such cases.

Within the assumptions in the present analysis, $\Delta \bar{F}_0$ remains continuous for a pressure field perturbation containing a discontinuity such as a shock wave, provided the shock wave is approximated as normal to the wing surface. More precisely, geometry slope $\Delta(\mathrm{d}\bar{F}_0/\mathrm{d}x)$ is proportional to Δw, the velocity perturbation correction normal to the surface, and it remains constant across the shock wave.

A discretized numerical formulation is formulated to approximate the integral equation and the resulting linear system is solved easily by standard techniques such as the Gaussian elimination method. The present geometry correction code is named WINDES.

Navier-Stokes Code

The Navier-Stokes code utilized in the present design procedure is a two-dimensional airfoil analysis code NSFOIL.[25] It is based on the implicit approximate factorization scheme for the time-dependent compressible time-averaged Navier-Stokes equations originally developed by Beam and Warming[26] and Steger.[27] The treatment of the internal boundary on the airfoil surface and the wake is improved, as it is treated implicitly. The time step is given as a monotonically increasing hyperbolic tangent function of the iterative step number for the time-accurate analysis. The Courant number of the initial time step is less than unity and the final time step is limited by the nonlinear stability and physical scale of time. It is important that the time step be asymptotically increased to the final time step. An abrupt change of time step leads to numerical instability. As the code must be applied to arbitrary geometry in the present design procedure, robustness of the analysis code is a necessary requirement. For turbulent boundary-layer and wake evaluations, the Baldwin-Lomax turbulence model is used.

The present code has been extensively applied to the analysis of various supercritical airfoils at a wide range of flow conditions and favorably compared with the experimental results from tests performed in the NAL high Reynolds number two-dimensional transonic wind tunnel.[28] The mesh system used by NSFOIL is generated by a body-fitted mesh generation code AFMESH.[29] AFMESH uses various combinations of mesh generating methods such as the elliptic equa-

tion, geometric construction, and algebraic sheared mesh methods. It incorporates many input options to generate the most appropriate mesh distribution for a particular airfoil the designer wants to apply. Therefore, NSFOIL and AFMESH are easily combined with the geometry correction code WINDES. The present design procedure programs as a unit, including those three codes and the various interface programs to connect them, will be referred to as TFPDNS, representing transonic full potential design utilizing Navier-Stokes equations.

Computed Results

Some of the computed results are presented for transonic and low-speed airfoil designs to demonstrate the practical applicability of procedure TFPDNS. For all of the two-dimensional airfoil design numerical examples, the three-dimensional design code WINDES is used as if we are designing a three-dimensional wing with an unswept rectangular planform of high aspect ratio (20) with the same pressure distribution and the same wing section geometry as the ones given by the two-dimensional analysis code NSFOIL. The root wing section geometry designed was used for the next analysis mode input. This was done to avoid reconstructing the two-dimensional design code from WINDES. Direct application of the three-dimensional design code does not hamper the validity of the procedure and the computed results for the airfoil design.

Case I: Shockless Airfoil Design

The first target is a shockless supercritical pressure distribution with lift coefficient $C_L = 0.6$. This target pressure distribution is actually a numerically obtained one by NSFOIL for the Garabedian-Korn airfoil 75-06-12 at its design condition: flow Mach number $M_\infty = 0.75$, angle of attack $\alpha = 0.8$ deg, and Reynolds number $Re = 1.3 \times 10^7$. A 125 × 51 C-type grid with 93 points on the airfoil surface is used throughout. The first grid point spacing adjacent to the surface is 1×10^{-5} of the chord length to cover the viscous sublayer resolution of flow at high Reynolds numbers. The far-field boundary is placed 12 chord lengths away from the airfoil. The pressure distribution is shockless at the design point as far as the present mesh resolution is applied.

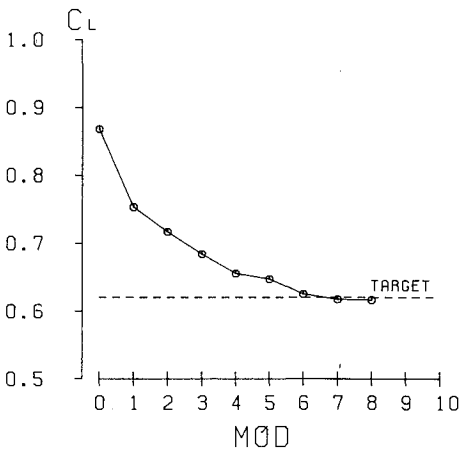

Fig. 1 History of lift coefficient, case I.

To start the design procedure, the same airfoil at angle of attack $\alpha = 2.0$ deg is selected as the initial geometry. The initial pressure distribution contains a strong shock wave and the lift coefficient is 0.87. During the iterative design procedure, the angle of attack in the analysis mode, as well as all of the other flow and computational parameters, is fixed to the same as in the initial mode. Only the coordinates of the airfoil are corrected by the design mode output and the computational mesh is reconstructed for the next analysis mode. The iterative history of the lift coefficient is shown in Fig. 1. The significant change of the lift coefficient is accomplished in the first four modes and, thereafter, the improvement at each mode becomes small. To understand how the correction proceeds, the geometry and pressure distribution at each iterative mode are examined. Some of the results are shown in Fig. 2 for modes 1, 3, and 5. In the figures, the designed geometry (solid line) is compared with the initial geometry (dashed line). The scale is exaggerated in the normal direction to illustrate the correction in the geometry. The corresponding pressure distributions are also shown in Fig. 2 using corresponding lines. It can be seen that a strong shock wave exists at the 65% chord station for the initial geometry. The target pressure distribution is also shown with symbol ●. It is clear that the geometry corrected at each design mode rotates gradually anticlockwise in the fixed computational space while retaining its analogy to the initial geometry. This is an expected result, since the initial geometry differs only in the angle of the attack by 1.2 deg from the target geometry and its shape is the same. The lower surface pressure distribution, where the flow is subcritical, converges with only one iteration. The upper surface negative peak pressure behind the leading-edge expansion also converges with one iteration. The pressure correction in the vicinity of the shock wave requires several iterative steps until the target pressure is attained. The figures show that the convergence of the pressure distribution is reached oscillatorily in the intermediate modes until the shock wave finally disappears.

A total of eight iterations produced the satisfactory result of attaining the target pressure distribution. The final geometry and the designed pressure distribution are shown in Fig. 3 using lines and symbols identical to those in Fig. 2. The geometries are depicted in normal scale. The local Mach

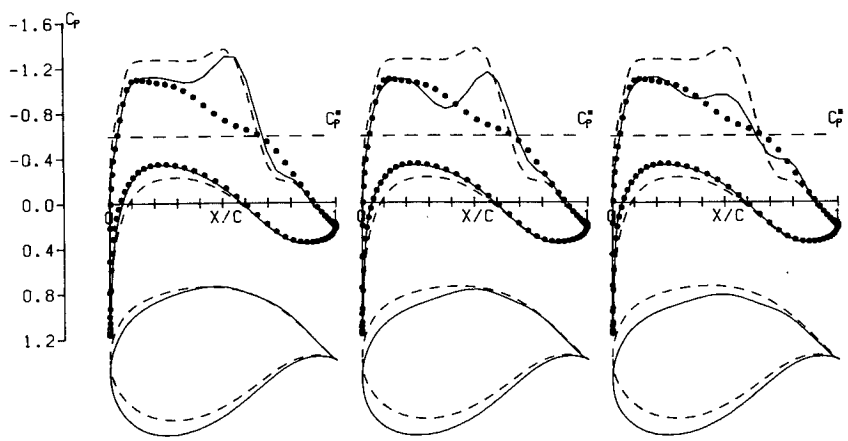

a) Mode 1. b) Mode 3. c) Mode 5.

Fig. 2 Iterative history of design and pressure recovery, case I (.... target, —— designed, and ---- initial).

number distributions around the designed and initial airfoils are shown in Figs. 4a and 4b, respectively. The dashed line represents the sonic line. A strong shock wave on the upper surface of the initial airfoil disappears on the designed airfoil. Boundary-layer characteristics such as the displacement thickness and form factor are computed and the designed airfoil has moderate characteristics when compared with the original. The boundary-layer growth behind the shock wave as seen in Fig. 4b is improved in Fig. 4a, the designed airfoil. The drag coefficient C_D is reduced by half from 0.026 to 0.013. The lift-to-drag ratio is improved by about 50% from 33 to 49.1. The skin-friction coefficient at the foot of the shock is scarcely positive in the original airfoil and significantly improved in the designed geometry.

The resolution of the flowfield, especially the shock wave and boundary layer in the Navier-Stokes code, depends on the total number and distribution of grid points along the surfaces. The spacing near the shock region in the flow direction is rather coarse in the present calculation. The shockless pressure distribution is attained within the present resolution. The accomplishment of the design target must be measured with the consideration of the resolution applied. In fact, the present airfoil was tested at the NAL wind tunnel and it was found that there exists a weak shock wave at the present flow condition. The adoption of a more refined mesh and solution adaptive mesh for the shock wave will give a more refined design.

Case II: Supercritical Airfoil Design

In the next case, a roof top supercritical pressure distribution on the upper surface is arbitrarily specified. The lower surface pressure distribution is the same as in case I. The lift coefficient target $C_{L\text{target}}$ is 0.7. The Garabedian-Korn airfoil at the design point is used as the initial airfoil geometry. The result shows that only two iterations give almost satisfactory designed lift coefficient $C_{L\text{designed}} = 0.69$. A total of four iterations is needed, however, to attain the target pressure distribution. The designed airfoil has a greater thickness and a larger camber distribution than the initial airfoil. The pressure distribution attained is shockless. The boundary layer separates at the 98% chord station on the upper surface in the present design. This trailing-edge separation is expected since the target pressure recovery in the aft part of the upper surface is severe in this case. The Navier-Stokes code produces an accurate forecast of separation without implementing any numerical gimmicks, unlike a full potential code. The design is accomplished with ease.

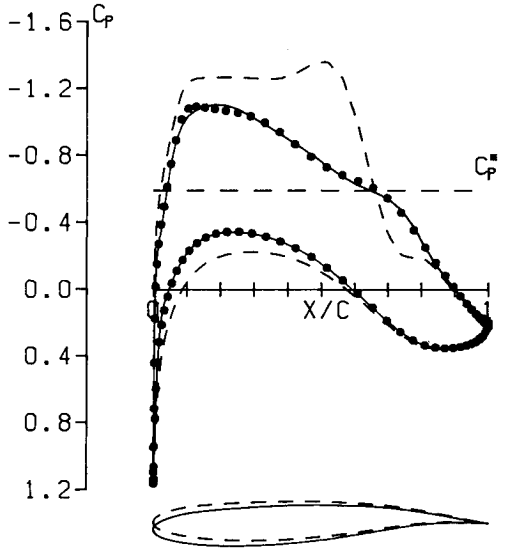

Fig. 3 Case I: shockless airfoil design result, comparison of pressure distributions and geometries.

Case III: Arbitrarily Specified Supercritical Design

The last supercritical design treats an arbitrarily specified pressure distribution on both sides of the surfaces with the lift coefficient $C_{L\text{target}} = 0.62$. The target pressure distribution is shown in Fig. 5 with symbol ●. The initial geometry and its pressure distribution are also shown with dashed lines. The flow condition is the same as before. The iterative history of geometry correction shows that the lower surface is corrected with 2 design modes, while the upper surface requires 10 design modes to attain satisfactory pressure recovery. A sharp pressure oscillation still remains in the vicinity of the leading edge, as shown in Fig. 5. The designed airfoil has a negative thickness in the region near the trailing edge because the initial airfoil has a thin cusp-type trailing edge. Therefore, the thickness distribution is modified so as to thicken proportionally to $\delta_{TE}\sqrt{x}$ evenly on both sides of the airfoil. The parameter δ_{TE} is the modified trailing-edge thickness and is equal to 0.0025 chord length. The pressure profile for the modified geometry remains unchanged except in the trailing-edge region where a small discrepancy appears due to the modification. The designed geometry and pressure distribution in Fig. 5 are from the present modified airfoil. The loss of the lift coefficient due to this modification is only 0.036. This is recovered by the increment in angle of attack of 0.12 deg without appreciable change in the pressure profile or the drag coefficient.

Case IV: Conventional Low-Speed Airfoil Design

The present procedure is also easily applicable to low-speed airfoil design. As an example, a conventional pressure distri-

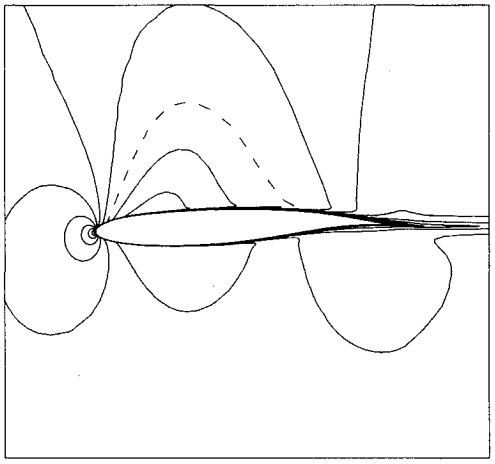

a) Designed geometry.

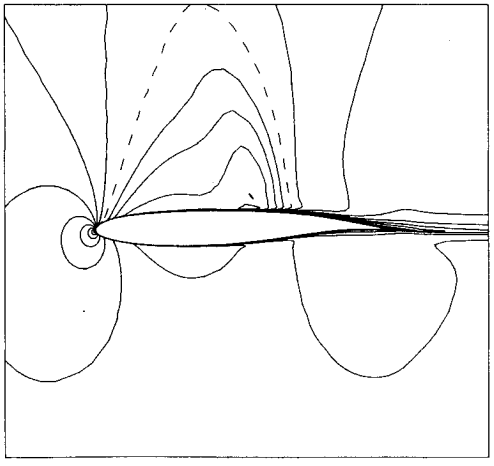

b) Initial geometry.

Fig. 4 Comparison of local Mach number distributions, case I.

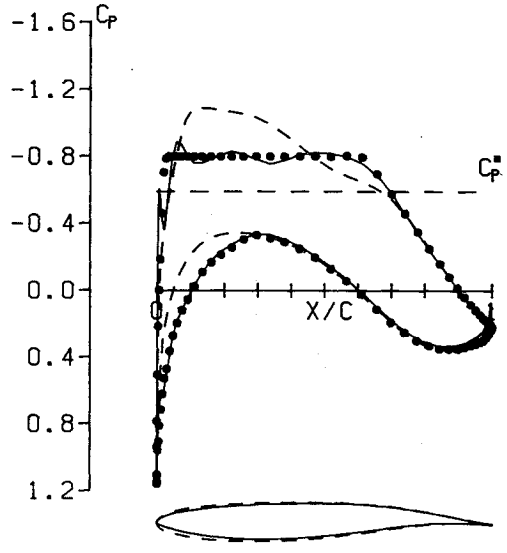

Fig. 5 Case III: arbitrarily specified supercritical design result.

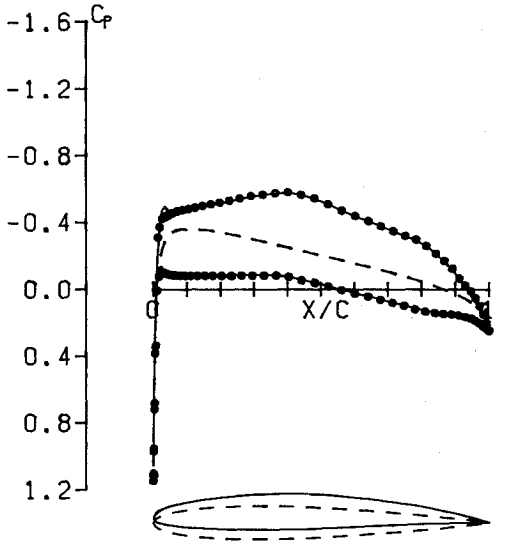

Fig. 6 Case IV: conventional low-speed airfoil design result.

bution with lift coefficient $C_L = 0.4$ is specified. The flow condition is as follows: flow Mach number $M_\infty = 0.4$, angle of attack $\alpha = 0$, and Reynolds number $Re = 3 \times 10^6$. For low-speed design, the effect of the outer boundary position is small and can be analytically compensated. Therefore, the computing region size is reduced to two chord lengths in each direction from the airfoil. The total number of grid points is 113×33. The mesh distribution in the vicinity of the airfoil is not changed from the previous cases. The mesh spacing along surface at the leading edge is 0.0025 chord length to properly evaluate the detail of the curvature distribution in the leading-edge region.

A NACA 0010 airfoil at zero angle of attack is chosen as the initial geometry. After three design modes, the pressure recovery is satisfactorily accomplished with the lift coefficient $C_L = 0.393$ as shown in Fig. 6. The designed airfoil has a maximum thickness-to-chord ratio of 0.11 and the geometry contour is similar to a conventional NACA 64 series airfoil.

Case V: Unconventional Low-Speed Airfoil Design

The last example shows the limit of applicability of the present procedure: a low-speed pressure distribution for a

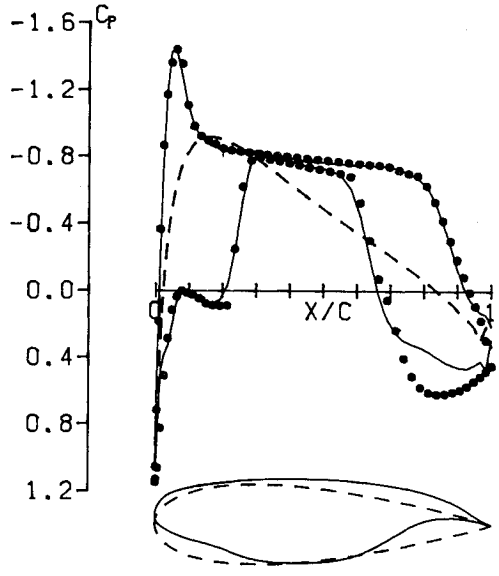

Fig. 7 Case V: unconventional low-speed airfoil design result.

thick airfoil that may be subject to trailing-edge separation. The flow condition is: flow Mach number $M_\infty = 0.4$, angle of attack $\alpha = 0$, Reynolds number $Re = 6 \times 10^6$, and lift coefficient $C_L = 0.6$. A NACA 0024 airfoil is used as the initial geometry. The lift coefficient $C_L = 0.56$ is attained at mode 3 with an excellent pressure recovery, except in the last 30% of chord on the lower surface where the rear loading requirement is severe. At the 65% chord station on the lower surface, a weak separation of the boundary layer occurs and the pressure recovery is not satisfied. More iteration results in a formation of an unrealistic geometry and considerable reverse flow, while the pressure recovery is not improved. Figure 7 shows the designed geometry at mode 3 with a trailing-edge thickness modification $\delta_{TE} = 0.0020$ and the attained pressure distribution as well as the initial and the target pressure distributions. The designed airfoil has maximum thickness to chord ratio 0.255.

From this result, it can be said that 1) thick airfoils are designed as well as thin and medium ones, 2) specification of an extraordinary pressure recovery leads to a large separation of flow, and 3) the assumption underlying the present procedure becomes invalid for such a situation. The design of attached flow will become a severe task even with the present procedure. The use of a Navier-Stokes code in the analysis mode, however, gives more details of the flow regime and a clue to improve for such cases when compared with the conventional methods.

Computing Resources

The computing time required for the present procedure is governed by the iterative step number times the analysis code run time. The CPU time for one design mode requires only 20 s, while one typical analysis run requires 90-110 min on a Fijitsu FACOM M-380. An appreciable reduction of CPU time is obtained when the converged flowfield of the previous analysis mode solution is used as the initial condition of the next analysis run, since the modification of the geometry is small at each design mode in most cases. As a result, a total CPU time of 4 h is required for case II, while 16 h is required for case I, in which the conventional impulsive start condition is applied.

This CPU time requirement may seem impractical for airfoil design. The object of the present work is to show the possibility of the design utilization of Navier-Stokes equations and is not aimed at an immediate practical procedure development. The work is preliminary and may be confined in a research

laboratory at the present time. Adoption of a local time step method and a multigrid method will further reduce the CPU time of the analysis code, although they were not applied in the present paper. Another innovative speed-up is expected with the introduction of the most advanced vector processing computer with performances faster than one giga FLOPS, which is to be installed at the National Aerospace Laboratory. A fifty times reduction of the run time is expected by the use of various vector coding techniques and algorithm improvements. Then, one airfoil design will be handled in less than 5 min, which is comparable to the conventional potential design procedure run time. Then, the only weak point in the present procedure—the CPU time requirement—will be considerably alleviated.

Conclusions

An iterative procedure for transonic airfoil design utilizing the Navier-Stokes equations to attain arbitrarily specified pressure distributions is proposed and numerical examples for transonic and low-speed airfoil designs are demonstrated to be effective. Since the Navier-Stokes equations are used in the analysis mode of the procedure, shock wave and viscous effects (including trailing-edge separation) are properly evaluated and effectively incorporated in the design that the conventional potential design methods have difficulty in evaluating.

Although the present work may be a preliminary one for use only in a research laboratory, the advanced vector processing computers, such as the FACOM VP-400 and the Cray 2, will make the present procedure practical. The extension of the procedure to three-dimensional wing design is straightforward. The procedure will also be suitably applicable to laminar flow control airfoil design. When the trend of computational fluid dynamics is toward three-dimensional Navier-Stokes analysis code development, a Navier-Stokes utilization for design procedure is cultivated.

References

[1]Boppe, C.W. and Stern, M.A., "Simulated Transonic Flow for Aircraft with Nacelles, Pylons, and Winglets," AIAA Paper 80-0130, 1980.

[2]Jameson, A. and Baker, T.J., "Solution of the Euler Equations for Complex Configurations," AIAA Paper 83-1929, 1983.

[3]Miyakawa, J. and Hirose, N., "The Comparison of the Transonic Airfoil Calculation by NSFOIL with the Wind Tunnel Test Data at High Reynolds Number," *Proceedings of 2nd NAL Symposium on Aircraft Computational Aerodynamics*, NAL SP-3, pp. 245–254, 1984 (see also, "Comparison of Transonic Airfoil Characteristics by Navier-Stokes Computation and by Wind Tunnel Test at High Reynolds Number," AIAA Paper 85-5025, 1985).

[4]Obayashi, S. and Fujii, K., "Computation of Three-Dimensional Viscous Transonic Flows with the LU Factored Scheme," AIAA Paper 85-1510, 1985.

[5]Slooff, J.W., "Computational Procedures in Transonic Aerodynamic Design," *Applied Computational Transonic Aerodynamics*, AGARD-AG-266, Aug. 1982, pp. 52–75.

[6]Hicks, R.M., "Transonic Wing Design Using Potential Flow Codes—Success and Failures," SAE Paper 810565, 1981.

[7]Cosentino, G.B. and Holst, T.L., "Numerical Optimization Design of Advanced Transonic Wing Configurations," AIAA Paper 85-0424, 1985 (see also, *Journal of Aircraft*, Vol. 23, March 1986, pp. 192–199).

[8]Zoutendijk, G., *Methods of Feasible Directions*, Elsevier, Amsterdam, 1960.

[9]Vanderplaats, G.N., "CONMIN: A FORTRAN Program for Constrained Function Minimization: User's Manual," NASA TM X-62282, Aug. 1973.

[10]Carlson, L.A., "Transonic Airfoil Design Using Cartesian Coordinates," NASA CR-2578, 1976.

[11]Tranen, T.L., "A Rapid Computer Aided Transonic Airfoil Design Method," AIAA Paper 74-501, 1974.

[12]Henne, P.A., "Inverse Transonic Wing Design Method," *Journal of Aircraft*, Vol. 18, Feb. 1981, pp. 121–127.

[13]Shanker, V., "A Full Potential Inverse Method Based on a Density Linearization Scheme for Wing Design," AIAA Paper 81-1234, 1981.

[14]Barger, R.L. and Brooks, C.W., "A Streamline Curvature Method for Design of Supercritical and Subcritical Airfoils," NASA TN D-7770, 1974.

[15]Davis, W.H. Jr., "Technique for Developing Design Tools from the Analysis Methods of Computational Aerodynamics," AIAA Paper 79-1529, 1979.

[16]McFadden, G.B., "An Artificial Viscosity Method for the Design of Supercritical Airfoils," Ph.D. Thesis, New York Univ., New York, 1979.

[17]Takanashi, S., "Iterative Three-Dimensional Transonic Wing Design Using Integral Equations," *Journal of Aircraft*, Vol. 22, Aug. 1985, pp. 655–660.

[18]Takanashi, S., "Transonic Wing and Airfoil Designs Using Inverse Code WINDES," *Proceedings of 3rd NAL Symposium on Aircraft Computational Aerodynamics*, NAL SP-5, 1985, pp. 251–256.

[19]Jameson, A. and Caughey, D.A., "Numerical Calculation of the Transonic Flow Past a Swept Wing," NASA CR-153297, 1977.

[20]Jameson, A. and Caughey, D.A., "A Finite Volume Method for Transonic Potential Flow Calculations," AIAA Paper 77-635, 1977.

[21]Boppe, C.W., "Transonic Flow Field Analysis for Wing-Fuselage Configurations," NASA CR-3243, 1980.

[22]Melnik, R.E., Mead, H.R., and Jameson, A., "A Multi-Grid Method for the Computation of Viscid/Inviscid Interactions on Airfoils," AIAA Paper 83-0234, 1983.

[23]Kamiya, N. and Hirose, N., "Research on Transonic Wings at the National Aerospace Laboratory, Japan," ICAS Paper 80-11-1, Oct. 1980.

[24]Takanashi, S., "Logical Concept of Transonic Wing Design Code WINDES," NAL TR, to be published.

[25]Kawai, N. and Hirose, N., "Development of the Code NSFOIL for Analyzing High Reynolds Number Transonic Flow around an Airfoil," NAL TR-816, 1984.

[26]Beam, R. and Warming, R.F., "An Implicit Finite-Difference Algorithm for Hyperbolic Systems in Conservation Law Form," *Journal of Computational Physics*, Vol. 22, 1976, pp. 87–110.

[27]Steger, J.L., "Implicit Finite Difference Simulation of Flow About Arbitrary Geometries with Application to Airfoils," AIAA Paper 77-665, 1977.

[28]Hirose, N., Kawai, N., Oguchi, K., and Kodera, T., "Validation and Comparison with Experiment of a High Reynolds Number Transonic Flow Airfoil Analysis Code NSFOIL," *Proceedings of 2nd NAL Symposium on Aircraft Computational Aerodynamics*, NAL SP-3, 1984, pp. 235–244.

[29]Hirose, N., Kawai, N., Isawa, T., and Kikuchi, M., "Development of Grid Generator Code AFMESH for Transonic Airfoil Analysis Codes," *Proceedings of 13th Annual Meeting, Japanese Society of Aeronautics and Space Sciences*, 1982, pp. 158–161,